Radar wind profiler signal characteristics during bird migration episodes

Volker Lehmann[1] and Gerd Teschke[2]

[1]Deutscher Wetterdienst, Meteorologisches Observatorium Lindenberg, Germany
[2]University of Applied Sciences, Neubrandenburg, Germany

ABSTRACT

The Gabor transform is used to investigate non-stationary wind profiler radar signals, which are frequently occurring during the seasonal bird migration. It is shown that the Gabor phase space representation contains a wealth of information and can be effectively used to separate the atmospheric signal component from the clutter. The crucial role of the dwell time as one of the primary sampling parameters of the wind profiler is discussed.

1. Introduction

Radar wind profilers (RWP) are being widely used for measuring wind velocities in the atmosphere. Recent reviews of the technical and scientific aspects of RWP including its signal processing have been provided by Gage (1990); Röttger and Larsen (1990); Doviak and Zrnic (1993) and Muschinski (2004). Especially the routine application by weather services and the assimilation of the data in Numerical Weather Prediction Models is an indicator for the success of this remote sensing technology, see e.g. Monna and Chadwick (1998); Bouttier (2001); Benjamin et al. (2004); St-James and Laroche (2005); Ishihara et al. (2006). However, the operational application is not without difficulties. Sometimes, comparisons with independent wind measurements show large and unacceptable differences between the profiler data and the reference. In many cases these differences are clearly attributable to either clutter echoes or Radio Frequency interference. Spurious signals are often easily discernible in the Doppler spectrum by human experts, but not always correctly handled by the automatic processing. For that reason, research on improvements in wind profiler signal processing has remained a very active field over the last decade.

In this paper we discuss some properties of intermittent clutter signals. This is of importance because echoes from migrating birds in spring and fall generate such clutter signals. Birds are effective targets for a wide range of radars from X-band to UHF (Vaughn, 1985; Bruderer, 1997) and therefore also a problem in wind profiling (Ecklund et al., 1990; Barth et al., 1994). The problem is well-known for more than a decade (Wilczak et al., 1995; Engelbart et al., 1998). The susceptibility of wind profiler radar systems to bird echoes depends primarily on wavelength and antenna characteristics. It mostly affects L-band and UHF-systems, that is Boundary Layer and Tropospheric profilers, as discussed in Wilczak et al. (1995). Intermittent clutter is an issue for both standard Doppler-beam swinging radars and imaging radar systems (Cheong et al., 2006; Chen et al., 2007). If present, such spurious signals can cause a significant deterioration of the quality of the derived winds. It is absolutely mandatory to avoid the assimilation of bird contaminated profiler wind data, as this can have significant effects on the quality of the forecasts (Semple, 2005).

The occurrence of intermittent clutter echoes makes it necessary to either use extensive quality control procedures to identify and skip contaminated data or to limit the data use to periods where bird migration is negligible. While the need for an extensive manual data quality control and cleaning might be acceptable for research activities, it is surely not feasible in any operational setting. Current state-of-the art profilers therefore run more or less sophisticated algorithms on site to reduce bird contamination (Merritt, 1995; Jordan et al., 1997; Ishihara et al., 2006), but practical experience supports the statement that the problem has not been fully resolved. It is therefore still an active research topic in RWP signal processing.

Recently, a new approach based on a redundant Gabor frame decomposition of the time series followed by the statistical filtering step has been suggested by Lehmann and Teschke (2008). While this method is capable of transient detection (for quality control) and has obviously a great potential for effective intermittent clutter filtering, preliminary results show that the sampling settings of the profiler, in particular the dwell time, are important for optimal clutter identification and

Further author information: Correspondence to: Volker Lehmann
E-mail: Volker.Lehmann@dwd.de, Telephone: +49 (0) 33677 60257
Address: Meteorologisches Observatorium, Am Observatorium 12, D-15848 Tauche OT Lindenberg

suppression during bird migration. In this paper we show that the Gabor frame decomposition method also provides hitherto unprecedented insight into the signal properties of the bird transients, because the time-frequency structure of the signal can be easily visualized through the Gabor spectrogram. This offers a new way of looking at the data beyond the raw time series and the Doppler spectrum and therefore provides opportunities for comprehensive investigation of the properties of meteorological and clutter signals.

2. The classical model of the radar raw signal

The classical RWP signal model assumption is that the demodulated discrete voltage sequence at the receiver output can be written as

$$\mathbf{S}[k] = \mathbf{I}[k]e^{i\omega k\Delta t} + \mathbf{N}[k], \tag{1}$$

where $\mathbf{I}[k] \sim N(0, \sigma_{\mathbf{I}}^2)$ and $\mathbf{N}[k] \sim N(0, \sigma_{\mathbf{N}}^2)$ are independent complex zero-mean Gaussian random vectors describing the atmospheric signal and the receiver noise, respectively (Zrnić, 1979), Δt is the sampling interval of the sequence and ω the mean Doppler frequency. Furthermore $\mathbf{I}[k]$ is narrowband compared to the receiver bandwidth and $|\omega| \leq \pi/\Delta t$ (Nyquist criterion). Because $\mathbf{S}[k]$ is the result of the demodulation of a real valued zero-mean and stationary Gaussian random process, the resulting Gaussian complex random process is also wide-sense stationary and zero-mean. Furthermore, the sequence has a vanishing pseudo-covariance, that is we have $\mathsf{E}(\mathbf{S}[k]\mathbf{S}[l]) = 0$.

Because $\mathbf{S}[k]$ is Gaussian, it is completely characterized through its covariance matrix R with entries

$$\begin{aligned}
(\mathsf{R})_{k,l} &= \mathsf{Cov}(\mathbf{S}[k], \mathbf{S}[l]) = \mathsf{E}(\mathbf{S}[k]\bar{\mathbf{S}}[l]) \\
&= \mathsf{E}(\mathbf{I}[k]\bar{\mathbf{I}}[l])e^{i\omega(k-l)\Delta t} + \mathsf{E}(\mathbf{N}[k]\bar{\mathbf{N}}[l]) \\
&= \sigma_{\mathbf{I}}^2 \rho[k-l]e^{i\omega(k-l)\Delta t} + \sigma_{\mathbf{N}}^2 \delta_{k-l,0},
\end{aligned}$$

where ρ is specified below. For the autocovariance function, we have

$$\mathsf{ACov}(k) = \sigma_{\mathbf{I}}^2 \rho[k] e^{i\omega k\Delta t} + \sigma_{\mathbf{N}}^2 \delta_{k,0} = \sigma^2 \rho[k] \ , \tag{2}$$

where we set

$$\sigma^2 := \sigma_{\mathbf{I}}^2 + \sigma_{\mathbf{N}}^2 \ \text{ and } \ \rho[k] := \frac{\sigma_{\mathbf{I}}^2 \rho[k] e^{i\omega k\Delta t} + \sigma_{\mathbf{N}}^2 \delta_{k,0}}{\sigma_{\mathbf{I}}^2 + \sigma_{\mathbf{N}}^2} \ .$$

The autocorrelation function $\rho[k]$ is typically assumed to follow a Gaussian correlation model, which corresponds to a Gaussian signal peak in the power spectrum. If the spectral width of the signal is w, then we have (Zrnić, 1979; Frehlich and Yadlowsky, 1994)

$$\rho[k] = e^{-2\pi^2 w^2 k^2 \Delta t^2} \ . \tag{3}$$

Note that this Gaussian correlation model must not be confused with the characterization of the random process as Gaussian, which covers a much wider class of signals. The assertions are normally very well justified and therefore often used in simulations of the radar signal (Zrnić, 1975; Frehlich and Yadlowsky, 1994; Muschinski et al., 1999). Furthermore, stationarity has to be assumed over typical dwell-times of $\mathcal{O}(1 \text{ minute})$. While this is a classical assumption in radar signal processing (Zrnić, 1975, 1979; Woodman, 1985; Frehlich and Yadlowsky, 1994; Lottman and Frehlich, 1997), it is typically unknown to which extent this assumption can be made safely. Apparently, this points to a rarely discussed problem in wind profiler signal processing, namely the (optimal) selection of dwell time T_d.

3. The problem of optimal dwell time

Wind profiler signal processing is by and large based on spectral estimation. The theory of spectral estimation in turn is closely related to the theory of stationary random processes. As a matter of fact, the basic motivation for studying the power spectrum of a stationary process is the Cramer spectral representation theorem. It states that every stationary random process can be decomposed into a sum of sinusoidal components with uncorrelated random coefficients. This is the analogue to the Fourier representation of deterministic functions (Priestley, 1981; Thomson, 1982; Brockwell and Davies, 1991; Percival and Walden, 1993). Of course one can also define the power spectrum as the Fourier transform of the autocovariance function of a process, but the interpretation through Cramer's theorem provides clearly more insight.

For nonstationary processes, it is certainly possible to compute a power spectrum but its interpretation will be difficult, if not impossible, because the spectrum alone will not suffice to fully describe the process as in the case for stationary processes. The calculation of a Doppler (power) spectrum for a nonstationary receiver signal necessarily leads to a loss of information, because phase relations between frequency components are suppressed [*]. One must conclude that stationarity of the radar receiver signal for some time interval (often termed quasi-stationarity or almost stationarity) has necessarily to be assumed if the estimation of the Doppler spectrum is to make sense. This instantly prompts again for the question of dwell time.

We follow Lottman and Frehlich (1997) in the definition of dwell time as *the total observation time required for the non-parametric estimation of a Doppler spectrum*, this definition includes spectral (or incoherent) integration, but ignores signal processing time for convenience. Note that dwell time is defined differently by several authors, see e.g. Strauch et al. (1984).

It is known that one can obtain a meaningful and valid measurement of the Doppler shift with dwell times of 1 s as discussed in Muschinski (2004). On example is the so-called Turbulent Eddy Profiler (TEP) (Mead et al., 1998), where typical dwell times (selected after the measurement) are ranging from about 2 to 8 s. However, this is in some contrast to most wind profiling applications, where dwell times typically range from about 15 s (Böhme et al., 2004) to more than 100 s (Merceret, 2000), with values of around 30 s being most typical. This large variability is likely an indication that the selection of dwell time is usually not regarded as a big issue in practice. However, from a theoretical point of view, the situation is clearly unsatisfactory. Obviously, the statistics of the received signal can only be stationary for a limited amount of time (quasi-stationarity). The maximum time period for which stationarity can be assumed is unknown because this obviously depends on the (a-priori) unknown properties of the (turbulent) scattering medium.

Of course it is of interest to achieve the highest possible temporal resolution in the determination of the Doppler moments. However, determining the Doppler moments is a statistical estimation problem due to the ubiquitous presence noise in the raw data and this calls for longer observation times to reduce the estimation error to an acceptable value. Also, the minimum-resolvable spectrum width depends on dwell time, because the velocity resolution of the discrete Fourier spectrum is $\propto (T_d)^{-1}$. The advantage of using longer dwell times simply stems from the fact that first the errors of the moment estimators are indirectly proportional to the observation time or dwell time, e.g. (Woodman and Guillen, 1974) and second the spectral resolution is improved. The latter might also be required for the identification of narrow-band RFI.

Choosing the dwell time thus essentially balances time and frequency resolution and also accuracy and signal detectability; it is obviously largely depending on the signal-to-noise ratio of the signal and the desired frequency resolution. It appears that this interesting question has not adequately been addressed in the literature on profiler signal processing. A brief discussion of the problem can be found in Strauch et al. (1984). Basically they state that the contribution of dwell time to the estimated spectral width (Gossard et al., 1998; White et al., 1999) should be negligible. However, both the true spectral width of the radar signal and the possible deviations from its stationarity are unknown. It thus appears that an a-priori estimation of the optimal dwell time is not possible. We suggest that the simultaneous time-frequency analysis of the radar signal, as described in our paper, can be used to further investigate this problem.

4. Time-frequency signal representation using a Gabor frame approach

Although they contain exactly the same information, neither the pure time representation of a transient signal (the complex time series of the demodulated voltage signal at the receiver output), nor its (complex) Fourier transform as a pure frequency representation (spectrum) are optimal representations to analyze the information content of non-stationary signals. It is

[*] Note that even for stationary processes, a single signal realization can only be retrieved from the full (complex) Fourier spectrum.

therefore tempting to look for an intermediate representation that aims at the joint time-frequency structure of the data. This is especially important for filtering: If we are able to separate stationary and nonstationary signal components in such a representation, then we might be able to suppress the nonstationary clutter part while leaving the stationary signal component essentially intact.

A quite natural way to analyze a continuous signal simultaneously in time and frequency is provided by the windowed Fourier transform (WFT), see Gabor (1946); Daubechies (1992); Kaiser (1994); Mallat (1999). It is essentially an extension of the well-known Fourier transform, where time localization is achieved by a pre-windowing of the signal with a normalized window function $h \in \mathbb{L}^2(\mathbf{R})$. For any given function $S \in \mathbb{L}^2(\mathbf{R})$, the WFT is defined as

$$V_h S(\tau,\omega) = \int_{-\infty}^{+\infty} S(t)h(t-\tau)e^{-i\omega t}dt \ . \tag{4}$$

The operator V_h maps isometrically between $\mathbb{L}^2(\mathbf{R})$ and $\mathbb{L}^2(\mathbf{R}^2)$, that is a one-dimensional function/signal is with no loss of energy transformed via the WFT into a two-dimensional function depending on both time τ and frequency ω. The (τ,ω)-plane is called the time-frequency (TF) plane or briefly the phase space. This representation was suggested by Gabor (1946) to illustrate that *both time and frequency are legitimate references for describing a signal*. The squared modulus of $V_h S$ is called the spectrogram, denoted by

$$P_h S(\tau,\omega) = |V_h S(\tau,\omega)|^2 \ , \tag{5}$$

and provides a measure for the signal energy in the time-frequency neighborhood of the point (τ,ω) and thus insight about the time-frequency structure of S. The resolution in time and frequency is controlled by the window function $h(t)$, but due to Heisenberg's uncertainty relation, there is no arbitrary resolution in time and frequency simultaneously, i.e. a point-wise frequency description in time domain and a point-wise time description in frequency domain is impossible. Formally, one considers in the uncertainty context for some centralized signal h with $\|h\| = 1$, time and frequency variances

$$\sigma_t^2 = \int_{-\infty}^{+\infty} t^2 |h(t)|^2 dt \quad \sigma_\omega^2 = \frac{1}{2\pi}\int_{-\infty}^{+\infty} \omega^2 |\hat{h}(\omega)|^2 d\omega \tag{6}$$

for which the Heisenberg uncertainty relation yields

$$\sigma_t \cdot \sigma_\omega \geq \frac{1}{2} \ . \tag{7}$$

It can be shown, that equality in (7) is achieved when h is a translated, modulated or scaled version of the Gaussian function (equality means achieving optimal resolution in the time-frequency plane). Their time-frequency spread is visualized through a rectangle with widths σ_t and σ_ω in the TF-plane, this is called a Heisenberg box - see Figure 1.

Since the WFT is an isometry, the inversion of the map V_h is performed by its adjoint,

$$\begin{aligned}
\langle S,S\rangle_{\mathbb{L}^2(\mathbf{R})} &= \|S\|^2_{\mathbb{L}^2(\mathbf{R})} = \|V_h S\|^2_{\mathbb{L}^2(\mathbf{R}^2)} \\
&= \langle V_h S, V_h S\rangle_{\mathbb{L}^2(\mathbf{R}^2)} = \langle V_h^* V_h S, S\rangle_{\mathbb{L}^2(\mathbf{R})}
\end{aligned}$$

and therefore

$$S(t) = V_h^* V_h S(t) = \frac{1}{2\pi}\iint_{\mathbf{R}^2} V_h S(\tau,\omega)h(t-\tau)e^{i\omega t}d\omega d\tau \ . \tag{8}$$

This provides an analysis and synthesis method for signals with finite energy. For discrete signals, however, the continuous transforms (4) and (8) would create very redundant and inefficient representations of the signal, therefore discretized versions need to be developed. This leads to the concept of frames, which is detailed in Lehmann and Teschke (2008). For the problem at hand, however, those technical details can be omitted and it suffices to explain the spectrogram through the WFT (which is actually computed through a discrete frame).

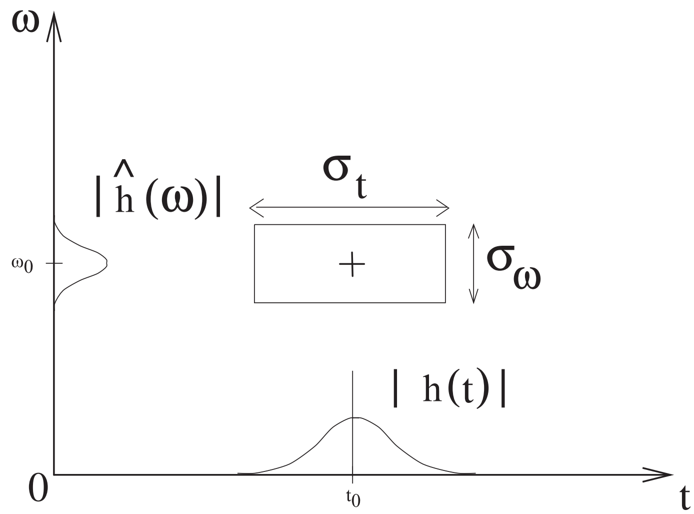

Figure 1. Schematic representation of the time-frequency plane and the Heisenberg-box (resolution) of the window function $h_{\tau,\omega}(t)$, centered at time $\tau = t_0$ and frequency $\omega = \omega_0$. Time resolution is indicated by σ_t, frequency resolution by σ_ω. The Heisenberg theorem states,that the area of the rectangle can never be smaller than 1/2.

5. Signal characteristics during bird migration

The classical signal model of equation (1) is widely used in theoretical considerations and usually quite adequate. As an example, we use the method of Zrnić (1975) to simulate a signal in line with the classical signal model, which contains only noise and a stationary atmospheric component. In the frequency domain, the atmospheric signal peak is assumed to be a Gaussian centered at $f_d = \omega/2\pi = -10.9s^{-1}$ and with a spectral width of $w = 0.9s^{-1}$. A discrete spectrogram of this signal is shown in Figure 2. The atmospheric signal component is represented as a horizontal line (stationarity) centered at the prescribed Doppler frequency. Noise is spread over the complete TF plane.

However, experience shows that the classical signal model must sometimes be extended by adding a clutter component (Muschinski et al., 2005):

$$\mathbf{S}[k] = \mathbf{I}[k]e^{i\omega k\Delta t} + \mathbf{N}[k] + \mathbf{C}[k] \; . \tag{9}$$

Clutter is by definition the totality of undesired echoes and interfering signals, therefore it is impossible to easily generalize the properties of $\mathbf{C}[k]$. In the case of RWP, clutter includes in particular echoes from airborne objects such as aircraft and birds as well as returns from the ground. Interfering signals may be caused by other radio transmitters operating in the RWP receiver band. In this paper, we restrict ourselves to intermittent clutter signals.

Examples of intermittent clutter signals have been published in a number of papers: Wilczak et al. (1995) described the distinct characteristic of bird contaminated I and Q data when seen in an A-scope display, but the shown time series taken with a 924 MHz RWP is only 0.5 s long, which is too short to see its essential characteristics. Jordan et al. (1997) show an example of a 30 s long time series taken with a 915 MHz RWP during bird migration, which exhibits a variation in the envelope of the signal due to modulation of signal amplitude by the antenna beam pattern. Another example of intermittent clutter caused by airplanes and a simple theoretical model is given by Boisse et al. (1999). The most distinct feature here is also the time-dependent amplitude of the signal. A 19 s time series of a 482 MHz RWP containing an airplane echo is discussed in Muschinski et al. (2005). When data containing intermittent clutter components are compared to both clear air and ground clutter signals (see Muschinski et al. (2005) for an example), it is very obvious, that the main difference is the transient character of the intermittent clutter signal component. Following Friedlander and Porat (1989), we define a transient signal as a signal whose duration is short to the observation interval, in our case the dwell time. Such a behavior clearly reflects a nonstationarity of the underlying scattering process.

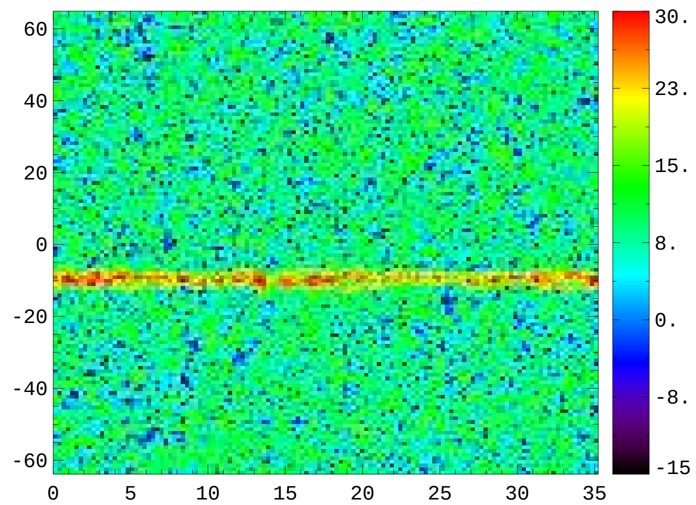

Figure 2. Gabor phase space representation of a simulated RWP signal containing only noise and a stationary signal component. The x-axis shows time (in seconds) and the y-axis frequency (in Hz). Color contours (logarithmic scaling in dB) denote the power of the Gabor coefficients.

While it is instructive to take a look at a few examples, it appears that the properties of the intermittent clutter component have not been investigated systematically.

In the autumn of 2005, time series data of the coherently integrated I/Q signal of the RWP at Bayreuth, Germany were saved in the wind low mode to get a unique dataset for the investigation of bird migration. For October 13, it was subjectively judged that the data showed a maximum of bird echoes. This day was therefore selected as a test case for the algorithm proposed by Lehmann and Teschke (2008). The time series (not shown here) have a length of about 35 s and the nonstationarity of the observed clutter echoes is striking. However, during reprocessing of the complete dataset it was revealed that the dwell time used was apparently rather short to guarantee that every observed intermittent clutter signal indeed exhibits a clear transient behavior. Sometimes the duration of the clutter signal component was on the order of the dwell time instead. If this is the case, then signal separation may fail and filtering may become challenging.

A systematic investigation seems therefore to be necessary. The difficulty is of course the large data amount of the time series. For the 482 MHz wind profiler of DWD, the daily file size of only the low mode data is about 3 Gigabyte. The development of an automated and efficient processing thus is a prerequisite for such a task. First test data were obtained during the bird migration season in autumn in Eastern Germany on October 26, 2007. Note that this special measurement used a comparably long dwell time of 166.6 seconds. Let us consider two examples from this dataset:

Figure 3 shows the time series obtained for the range gate centered at 624 m agl, and the corresponding Gabor phase space representation is shown in Figures 4. Several transients of different strength can be seen in the time representation, the strongest occurs at about 55 s into the dwell. The Gabor spectrogram reveals a number of additional interesting features: The transients are clearly visible and widely scattered in the TF-plane, with the strongest one having a signal power of almost 130 dB. Note that the linear dynamic range of the radar is limited to about 90 dB. Besides the intermittent clutter signals, an atmospheric return is visible at a frequency of about -10 Hz. Additionally, a weaker and spectrally narrow ground clutter return can be seen at zero Doppler frequency. Both the atmospheric and the ground clutter signal components are approximately stationary over the full length of the dwell.

Another example is shown in Fig 5 (time series) and Fig 6 (Gabor spectrogram). This was obtained at the range gate centered at about 2796 m agl with the dwell starting at 20:58:32 UTC. Remarkable is here the duration of the strong transient, which is on the order of the dwell times typically used in routine wind profiling. The spectrogram shows the atmospheric signal component as a quasi-stationary (horizontal) line at a frequency of about -2 Hz. If the dwell time would have been much shorter (e.g. about 30 s, a typical value in routine operation) and furthermore by chance coincide with the

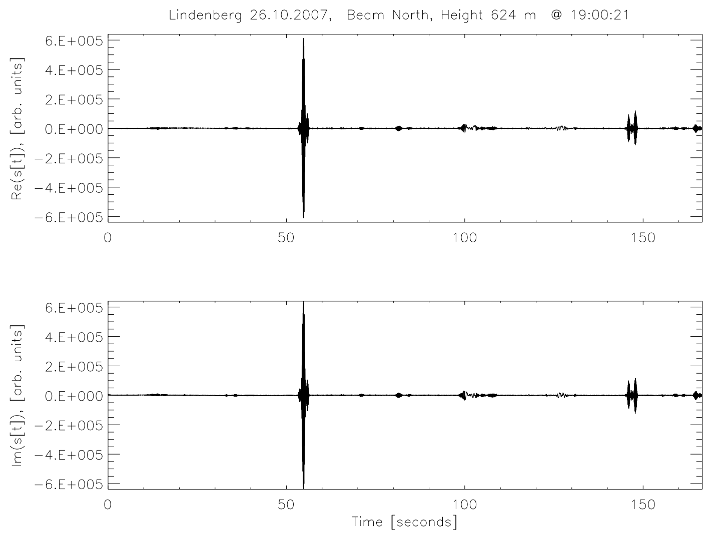

Figure 3. Demodulated receiver signal of the 482 MHz wind profiler at Lindenberg, obtained during bird migration on Oct 26, 2007. The total length of the time series is 166.6 s.

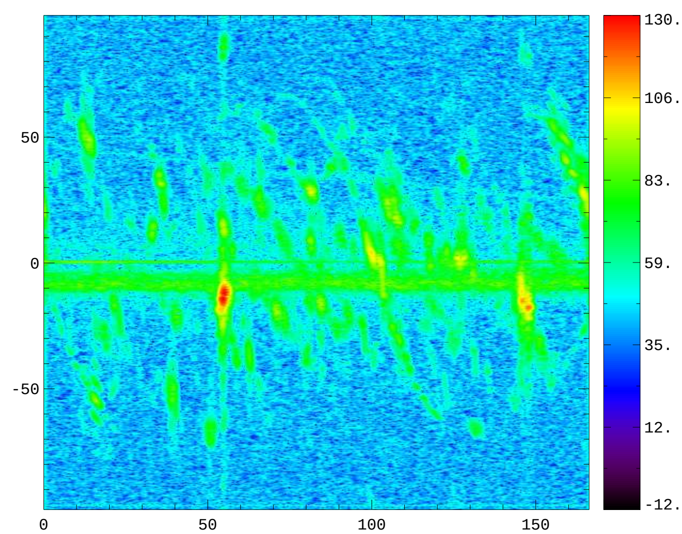

Figure 4. Time-Frequency analysis (Gabor spectrogram) of the signal shown in Fig 3. The x-axis shows time (in seconds) and the y-axis frequency (in Hz). Color contours (logarithmic scaling in dB) denote signal power. Frequent, but short bird transients of varying strength are visible.

bird event, it would have been extremely difficult, if not impossible, to identify the atmospheric return. Only a thresholding based on signal power could then be attempted to flag the data as invalid.

Both examples show that more work is indeed needed to investigate the typical signal properties during bird migration episodes, to be able to optimize both processing and sampling settings for operational radar wind profiler systems. The long-standing theoretical question of an optimal dwell time length in wind profiler operation thus becomes a new practical relevance.

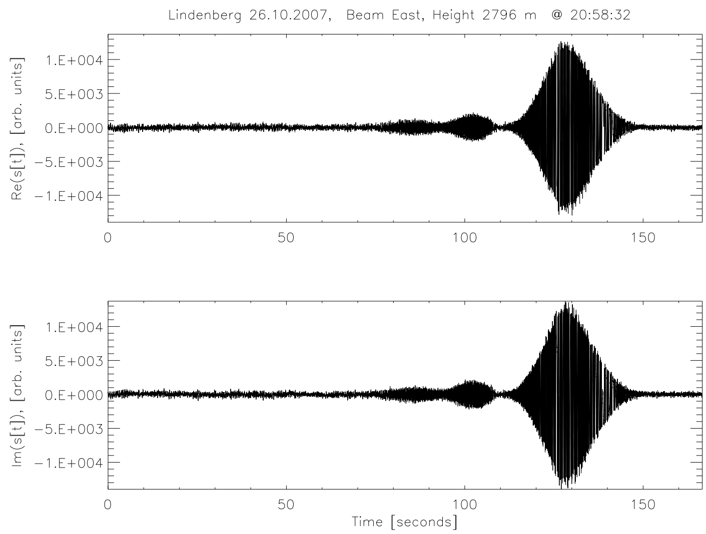

Figure 5. Demodulated receiver signal of the 482 MHz wind profiler at Lindenberg, obtained during bird migration on Oct 26, 2007. The total length of the time series is 166.6 s.

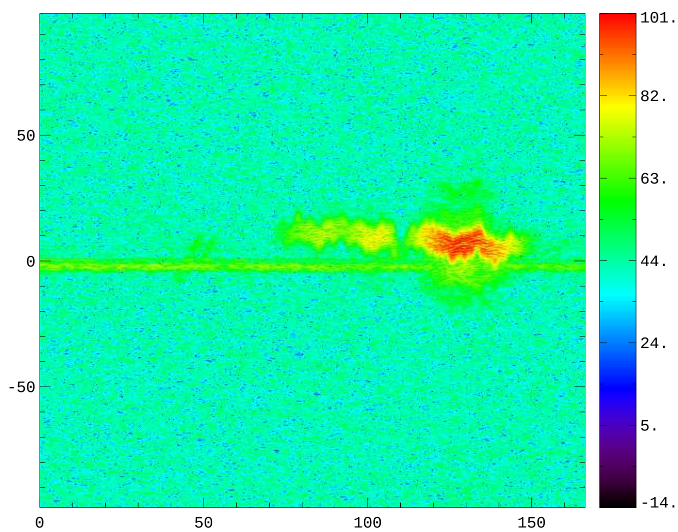

Figure 6. Time-Frequency analysis (Gabor spectrogram) of the signal shown in Fig 5. The x-axis shows time (in seconds) and the y-axis frequency (in Hz). Color contours (logarithmic scaling in dB) denote signal power. Note the strong bird transient, having a total duration of about 90s. The maximum signal power occurs for about 30 s, which is the same order as the typically used dwell times in routine wind profiling.

References

Barth, M., Chadwick, R., and van de Kamp, D., Data processing algorithms used by NOAA's wind profiler demonstration network, *Ann. Geophys.*, *12*, 518–528, 1994.

Benjamin, S. G., Schwartz, B. E., Szoke, E. J., and Koch, S. E., The value of wind profiler data in U.S. weather forecasting, *B. Am. Meteorol. Soc.*, pp. 1871–1886, 2004.

Böhme, T., Hauf, T., and Lehmann, V., Investigation of short -period gravity waves with the Lindenberg 482 MHz tropospheric wind profiler, *Q.J.R. Meteorol. Soc.*, *130*, 2933–2952, 2004.

Boisse, J.-C., Klaus, V., and Aubagnac, J.-P., A wavelet transform technique for removing airplane echos from ST radar signals, *J. Atmos. Ocean. Tech.*, *16*, 334–346, 1999.

Bouttier, F., The use of profiler data at ECMWF, *Meteorol. Z.*, *10*, 497–510, 2001.

Brockwell, P. J. and Davies, R. A., *Time Series: Theory and Methods*, Springer, 1991.

Bruderer, B., The study of bird migration by radar part 1: The technical basis, *Naturwissenschaften*, *84*, 1–8, 1997.

Chen, M.-Y., Yu, T.-Y., Chu, Y.-H., Brown, W. O., and Cohn, S. A., Application of Capon technique to mitigate bird contamination on a spaced antenna wind profiler, *Radio Sci.*, *42*, doi:10.1029/2006RS003 604, 2007.

Cheong, B., Hoffman, M., Palmer, R., Frasier, S. J., and Lopez-Dekker, F., Phased-array design for biological clutter rejection: Simulation and experimental validation, *J. Atmos. Ocean. Tech.*, *23*, 585–598, 2006.

Daubechies, I., *Ten Lectures on Wavelets*, SIAM, Philadelphia, 1992.

Doviak, R. J. and Zrnic, D. S., *Doppler Radar and Weather Observations*, Academic Press, 1993.

Ecklund, W., Carter, D., Balsley, B., Currier, P., Green, J., Weber, B., and Gage, K., Field tests of a lower tropospheric wind profiler, *Radio Sci.*, *25*, 899–906, 1990.

Engelbart, D., Görsdorf, U., and Ruhe, W., Effects and observation of migrating birds on a Boundary-Layer Windprofiler in Eastern Germany, *Meteorol. Z.*, *NF 7*, 280–287, 1998.

Frehlich, R. and Yadlowsky, M., Performance of mean-frequency estimators for doppler radar and lidar, *J. Atmos. Ocean. Tech.*, *11*, 1217–1230, 1994.

Friedlander, B. and Porat, B., Detection of transient signals by the Gabor representation, *IEEE T. Acoust. Speech.*, *ASSP-37*, 169–180, 1989.

Gabor, D., Theory of communication, *J. IEE (London)*, *93*, 429–457, 1946.

Gage, K. S., Radar observations of the free atmosphere: Structure and dynamics, in *Radar in Meteorology*, edited by D. Atlas, pp. 534–565, Amer. Meteor. Soc., Boston, 1990.

Gossard, E., Wolfe, D., Moran, K., Paulus, R., Anderson, K., and Rodgers, L., Measurement of clear-air gradients and turbulence properties with radar wind profilers, *J. Atmos. Oceanic Technol.*, *15*, 321–342, 1998.

Ishihara, M., Kato, Y., Abo, T., Kobayashi, K., and Izumikawa, Y., Characteristics and performance of the operational wind profiler network of the Japan Meteorological Agency, *J. Meteorol. Soc. Jpn.*, *84*, 1085–1096, 2006.

Jordan, J. R., Lataitis, R. J., and Carter, D. A., Removing ground and intermittent clutter contamination from wind profiler signals using wavelet transforms, *J. Atmos. Ocean. Tech.*, *14*, 1280–1297, 1997.

Kaiser, G., *A Friendly Guide to Wavelets*, Birkhäuser, Basel, 1994.

Lehmann, V. and Teschke, G., Advanced Intermittent Clutter Filtering for Radar Wind Profiler: Signal Separation through a Gabor Frame Expansion and its Statistics, *Ann. Geophys.*, *26*, 759–783, 2008.

Lottman, B. and Frehlich, R., Evaluation of Doppler radar velocity estimators, *Radio Sci.*, *32*, 677–686, 1997.

Mallat, S., *A Wavelet Tour of Signal Processing*, Academic Press, 1999.

Mead, J. B., Hopcraft, G., Frasier, S. J., Pollard, B. D., Cherry, C. D., Schaubert, D. H., and McIntosh, R. E., A volume-imaging radar wind profiler for atmospheric boundary layer turbulence studies, *J. Atmos. Oceanic Technol.*, *15*, 849–859, 1998.

Merceret, F. J., The coherence time of midtropospheric wind features as a function of vertical scale from 300 m to 2 km, *J. Appl. Meteorol.*, *39*, 2409–2420, 2000.

Merritt, D. A., A statistical averaging method for wind profiler Doppler spectra, *J. Atmos. Ocean. Tech.*, *12*, 985–995, 1995.

Monna, W. A. and Chadwick, R. B., Remote-sensing of upper-air winds for weather forecasting: Wind-profiler radar, *B. World Meteorol. Organ.*, *47*, 124–132, 1998.

Muschinski, A., Local and global statistics of clear-air Doppler radar signals, *Radio Sci.*, *39*, doi:10.1029/2003RS002 908, 2004.

Muschinski, A., Sullivan, P. P., Wuertz, D. B., Hill, R. J., Cohn, S. A., Lenschow, D. H., and Doviak, R. J., First synthesis of wind-profiler signals on the basis of large-eddy simulation data, *Radio Sci.*, *34*, 1437–1459, 1999.

Muschinski, A., Lehmann, V., Justen, L., and Teschke, G., Advanced radar wind profiling, *Meteorol. Z.*, *14*, 609–626, 2005.

Percival, D. B. and Walden, A. T., *Spectral Analysis for Physical Applications*, Cambridge University Press, 1993.

Priestley, M., *Spectral Analysis and Time Series*, Academic Press, 1981.

Röttger, J. and Larsen, M., UHF/VHF radar techniques for atmospheric research and wind profiler applications, in *Radar in Meteorology*, chap. 21a, pp. 235–281, American Meteorological Society, Boston, 1990.

Semple, A., Forecast error investigation 12th October 2003: Assimilation of contaminated wind profiler data into the global model (Forecasting Research Technical Report No. 465), Tech. rep., UK Met Office, 2005.

St-James, J. S. and Laroche, S., Assimilation of wind profiler data in the Canadian Meteorological Centre's analysis system, *J. Atmos. Ocean. Tech.*, *22*, 1181–1194, 2005.

Strauch, R. G., Merritt, D. A., Moran, K. P., Earnshaw, K. B., and van de Kamp, D., The Colorado wind profiling network, *J. Atmos. Ocean. Technol.*, *1*, 37–49, 1984.

Thomson, D. J., Spectrum estimation and harmonic analysis, *Proc. IEEE*, *70*, 1055–1096, 1982.

Vaughn, C. R., Birds and insects as radar targets: A review, *P. IEEE*, *73*, 205–227, 1985.

White, A., Lataitis, R., and Lawrence, R., Space and time filtering of remotely sensed velocity turbulence, *J. Atmos. Oceanic Technol.*, *16*, 1967–1972, 1999.

Wilczak, J., Strauch, R., Ralph, F., Weber, B., Merritt, D., Jordan, J., Wolfe, D., Lewis, L., Wuertz, D., Gaynor, J., McLaughlin, S., Rogers, R., Riddle, A., and Dye, T., Contamination of wind profiler data by migrating birds: Characteristics of corrupted data and potential solutions, *J. Atmos. Ocean. Tech.*, *12*, 449–467, 1995.

Woodman, R. F., Spectral moment estimation in MST radars, *Radio Sci.*, *20*, 1185–1195, 1985.

Woodman, R. F. and Guillen, A., Radar observation of winds and turbulence in the stratosphere and mesosphere, *J. Atmos. Sci.*, pp. 493–505, 1974.

Zrnić, D. S., Simulation of weatherlike Doppler spectra and signals, *J. Appl. Meteorol.*, *14*, 619–620, 1975.

Zrnić, D. S., Estimation of spectral moments for weather echoes, *IEEE T. Geosci. Elect.*, *GE-17*, 113–128, 1979.